Thin Solid Films 670 (2019) 54–59

Contents lists available at ScienceDirect

Thin Solid Films

journal homepage: www.elsevier.com/locate/tsf

TiN diffusion barrier for stable W/SiC(0001) interfaces in inert ambient at high temperature

Steven DelaCruz[a], Zhongtao Wang[a,b], Ping Cheng[a,c], Carlo Carraro[a], Roya Maboudian[a,*]

[a] Department of Chemical and Biomolecular Engineering, University of California at Berkeley, Berkeley, CA 94720, USA
[b] State Key Laboratory of Advanced Welding and Joining, Harbin Institute of Technology, Harbin 150001, People's Republic of China
[c] National Key Laboratory of Science and Technology on Micro/Nano Fabrication, School of Electronic Information and Electrical Engineering, Shanghai Jiao Tong University, Shanghai 200240, People's Republic of China

ARTICLE INFO

Keywords:
Titanium nitride
Tungsten
Silicon carbide
Sputtering
Diffusion barrier
Annealing
X-ray diffraction
Thermionic energy converter

ABSTRACT

The effect of high-temperature annealing on tungsten (W) films deposited on silicon carbide (SiC) with and without a titanium nitride (TiN) diffusion barrier was examined as a function of time. Evolutions in phase composition, surface morphology, and roughness from annealing at 1273 K were investigated for up to 24 h. Without a TiN diffusion barrier, solid state reactions between the W film and SiC substrate led to the formation of W_5Si_3, W_2C, and WC species and the rise of an inhomogeneous surface structure that was initially web-like and later discontinuous. Severe roughening on the order of the initial film thickness was observed. Incorporation of a 100 nm TiN diffusion barrier suppressed the formation of W_5Si_3 and W_2C and only trace WC could be detected due to species diffusion through TiN grain boundaries. Changes in the surface structure and roughness were minimal. The results of this work warrant consideration of TiN as an effective diffusion barrier for W on SiC systems where structural stability at high temperatures is highly desired.

1. Introduction

The tungsten (W)/silicon carbide (SiC) system has attracted much interest in recent years due to its importance to a number of technologies, ranging from gas-cooled fusion systems [1] and thermionic energy converters (TECs) [2] to high temperature and high power electronics [3]. Since many of these applications involve operation at high temperatures, several studies have reported the effects of annealing on the W/SiC system [1,3–9]. These studies have shown that elevated temperatures enhance the rate of solid-state reactions at the interface between W and SiC, yielding a variety of silicides and carbides. The formation of these compounds usually has negative impacts on the desired characteristics of the system. For example, they result in increased contact resistance between W and SiC [3], and in some cases, mechanical failures such as delamination or embrittlement [1,2].

To address these issues, it is necessary to incorporate a diffusion barrier between W and SiC to suppress the interfacial reaction. Due to its good electrical conductivity, high melting point, and large negative enthalpy of formation that grants stability to several materials, titanium nitride (TiN) has been demonstrated as an effective barrier in various metallization schemes (Al [10], Cu [11], Ag [12], W [13], etc.) to Si at elevated temperatures. Considering the W/SiC system, TiN exhibits thermodynamic stability to W up to 2173 K under vacuum conditions [14]. Limited studies of TiN films grown directly on SiC substrates [15–18], primarily for the purpose of metal contacts, also suggest non-reactivity of TiN to SiC up to at least 1373 K [18]. Thus, TiN satisfies the necessary requirement of being thermodynamically stable toward both W and SiC and holds promise as a diffusion barrier. However, few studies thus far have probed the barrier performance of TiN in metal/TiN/SiC systems. In the preparation of reinforced metal matrix composites, chemical-vapor deposited (CVD) TiN was shown to suppress the reaction between SiC fibers and a W-Cu alloy [19], and SiC particles and an Fe-based alloy [20]. Thick CVD TiN films (> 10 μm) have also been demonstrated as a stable barrier between a W substrate and CVD SiC film at high temperatures [21]. However, for several applications such as TECs and high-temperature electronics, it is more relevant to examine the behavior of TiN as a diffusion barrier between a SiC substrate and W thin film. This system is the focus of the present study. Additionally, in contrast to the aforementioned metal/TiN/SiC studies, we utilize a sputtering process for TiN, which is generally safer and avoids the toxic $TiCl_4$ precursor often employed in the TiN CVD processes. We report that a sputtered TiN thin film creates a high-temperature stable system between a W thin film and 4H-SiC(0001) substrate, which is the most commonly used wafer for SiC-based

* Corresponding author.
E-mail address: maboudia@berkeley.edu (R. Maboudian).

https://doi.org/10.1016/j.tsf.2018.11.058
Received 19 July 2018; Received in revised form 5 November 2018; Accepted 28 November 2018
Available online 29 November 2018

technologies. A temperature of 1273 K was examined for this study as it is an appropriate and frequently examined temperature for potential thermionic emitters [22–25].

2. Experimental details

Hexagonal 4H-SiC (0001) wafers (100 mm diameter, 365 μm thick, engineering-grade, 4° off-axis cut toward [1120], n-doped with 0.0195–0.0205 Ω·cm resistivity range, and low micropipe density of ≤5 micropipes/cm^2) were obtained as starting material (SiCrystal AG). Prior to deposition, substrates underwent a cleaning protocol, whereby they were sonicated in separate acetone and isopropanol baths, treated with ultraviolent ozone, rinsed in dilute hydrofluoric acid followed by deionized water, and dried with nitrogen gas.

TiN thin films were deposited onto clean 4H-SiC(0001) substrates using DC reactive sputtering of a Ti target (MRC 944 sputtering system). The base pressure of the system was 6.7×10^{-5} Pa. Pre-sputtering at 2 kW and an Ar pressure of 1.1 Pa was done for 2 min to clean the Ti target. This was followed by sputter etching at 200 W and an Ar pressure of 1.6 Pa for 2 min to remove potential contaminants from the SiC surface and improve the quality of the deposited films. TiN reactive sputtering was carried out at 2 kW and 1.1 Pa under 25% N_2/75% Ar flow until 100 nm films were obtained. W films were then deposited onto both the TiN/SiC samples and bare SiC substrates for parallel processing and comparison. W sputtering was carried out at 500 W and 1.1 Pa under Ar flow until 100 nm films were obtained. These film thicknesses were verified via cross-sectional imaging.

Annealing studies were conducted inside a hot-wall tube furnace (Thermo Scientific Lindberg Blue M) that was pumped to a base pressure of 1.3 Pa, wherein the W/SiC and W/TiN/SiC samples were heated to 1273 K at an average rate of ~50 K/min under 215 sccm Ar (Praxair, 99.999%) flow. The operating pressure was 130 Pa. Samples were held at 1273 K for a specific length of time (1 h, 5 h, or 24 h), after which the samples were gradually cooled back to room temperature under Ar flow.

Reaction products and crystallite properties for the W/SiC and W/TiN/SiC systems before and after annealing were characterized using X-ray diffraction (XRD, Bruker AXS D8 Discover with GADDS). Analysis was performed using a Co K_α radiation source and a step size of 0.005°. Phases and orientations were identified by comparing the obtained spectra to the International Centre for Diffraction Data database (ICDD-PDF-4). Changes in surface morphology were examined using scanning electron microscopy (SEM, FEI Quanta, accelerating voltage set to 20 kV). The evolution of surface roughness with annealing time was characterized using atomic force microscopy in tapping mode (AFM, Bruker Icon Scanning Probe Microscope).

3. Results and discussion

Phase identification with XRD was conducted to characterize the stability of the W/SiC(0001) system in the absence and presence of a TiN diffusion barrier. Different periods of annealing were examined to identify initial phase formation and the evolution of the reaction products with time. Fig. 1 compares the XRD patterns of the W/SiC and W/TiN/SiC samples as-deposited and after annealing at 1273 K for 1, 5, and 24 h. First considering the case without a TiN diffusion barrier, the as-deposited W/SiC sample is characterized by a high intensity diffraction peak at 46.9° corresponding to the (110) crystal planes of W. Minor peaks at 68.5° and 87.2° are attributed to the (200) and (211) planes of W, respectively, and highlight the polycrystalline nature of the sputtered film. No other peaks were observed, indicating the reaction kinetics at the W/SiC interface are relatively low during deposition. Comparison of the annealed W/SiC spectra reveal a dependence of the reaction products detectable by XRD on the time annealed. For the sample annealed for 1 h, several peaks characteristic of W_5Si_3 are observed. The most intense peaks are located at 42.3° (002), 44.9° (321),

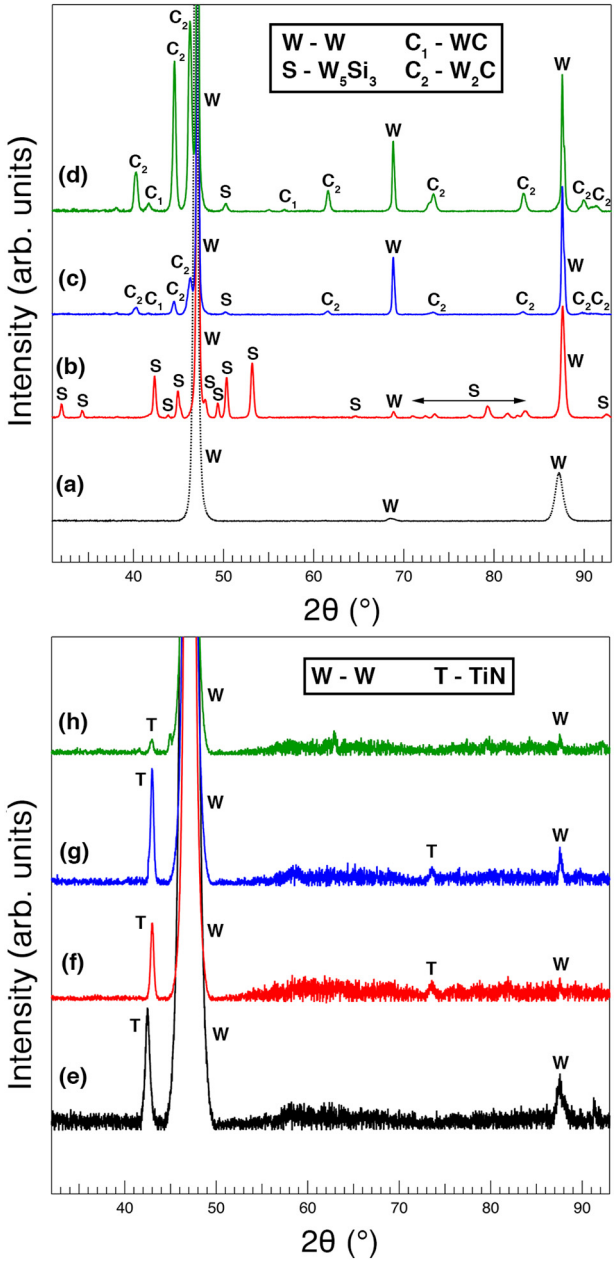

Fig. 1. (Top) XRD patterns of W/SiC samples (a) as-deposited and annealed at 1273 K for (b) 1 h, (c) 5 h, and (d) 24 h. (Bottom) XRD patterns of W/TiN/SiC samples (e) as-deposited and annealed at 1273 K for (f) 1 h, (g) 5 h, and (h) 24 h samples. Spectra have been normalized to the W (110) reflection.

50.3° (411), and 53.2° (222). Though expected, neither WC nor W_2C peaks could be identified from the spectrum, suggesting these carbides may only be nanocrystalline or amorphous after 1 h. Significant changes occur for the 5 h annealed sample, for which only the (411) peak of W_5Si_3 remains. Moreover, peaks corresponding to W_2C and WC appear, indicating that further reaction between SiC and the tungsten compounds occurred during the extended annealing time. The strongest W_2C peaks are found at 40.3° (100), 44.5° (002), 46.3° (101), while a singular, weak WC peak is found at 41.7° (100). For the 24 h annealed sample, the WC and W_2C peaks increase in relative intensity and an additional WC peak can be observed at 56.8° (101). Thermodynamic calculations for the W-Si-C system conducted by Seng and Barnes [5] indicate that the formation of W_5Si_3 and WC is favored over that of WSi_2 and W_2C at 1273 K; however, the roles of annealing time, pressure, environment, or SiC polytype in the W/SiC reaction have not been

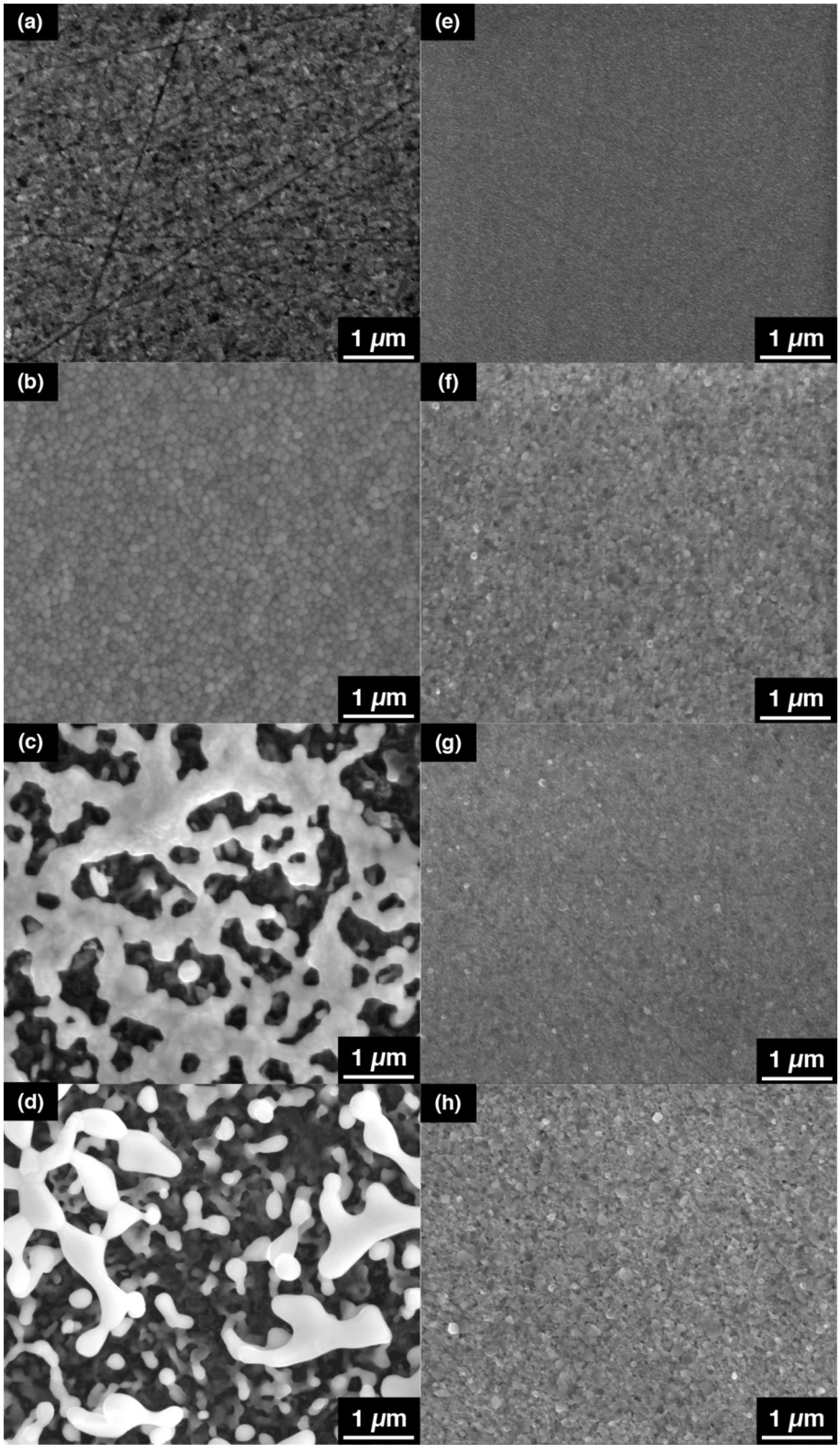

Fig. 2. (Left) SEM images of W/SiC samples (a) as-deposited and annealed at 1273 K for (b) 1 h, (c) 5 h, and (d) 24 h. (Right) SEM images of W/TiN/SiC samples (e) as-deposited and annealed at 1273 K for (f) 1 h, (g) 5 h, and (h) 24 h.

clearly established. Moreover, uncertainty regarding the stability of W_2C at room temperature exists among previous literature evaluations [3,6]. The absence of WSi_2 and formation of both W_5Si_3 and W_2C observed here most closely agree with the studies of Baud, et al. [6] (W on 3C-SiC, vacuum, 1373 K, 60 s) and Thabethe, et al. [9] (W on 6H-SiC, Ar, 1273 K, 1 h).

For the W/TiN/SiC samples, the as-deposited spectrum exhibits a dominant W peak at 47.1° (110) and a minor peak at 87.6° (211). The peak corresponding to the (200) planes of W is absent in the as-deposited and annealed spectra, unlike in the W/SiC samples where the

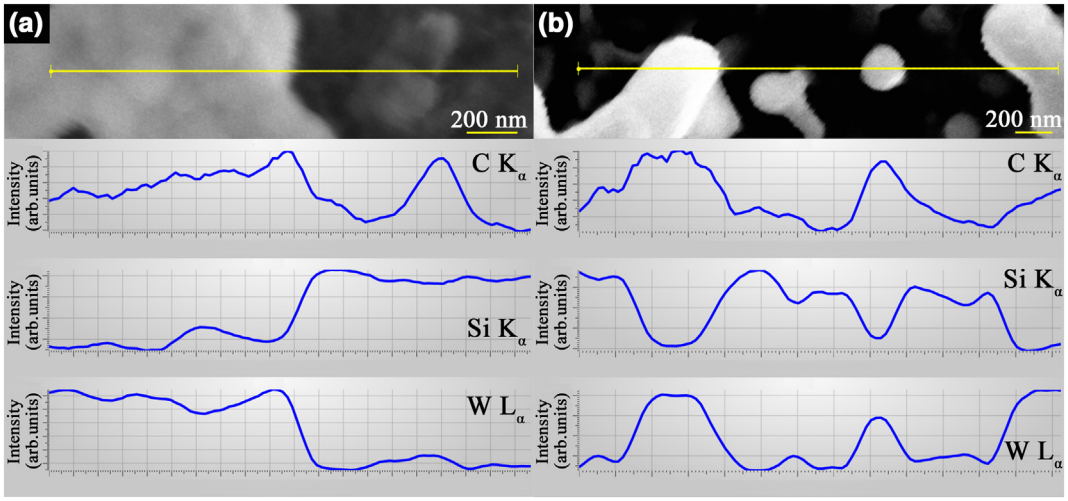

Fig. 3. EDS line scans showing C, Si, and W signals for the (a) 5 h annealed and (b) 24 h annealed W/SiC samples.

relative intensity of the (200) peak increases with annealing time. This suggests the underlying TiN layer influences the growth of the W layer during deposition or suppresses its evolution during the annealing process. The TiN interlayer is confirmed by the peak at 42.5° which corresponds to its (111) planes. For the 1 h annealed samples, an additional TiN peak at 73.6° (220) is observed. Few differences are observed between the 1 and 5 h annealed samples. For the 24 h annealed sample, the two TiN signals weaken drastically, with the (220) peak completely disappearing. Although not readily observable in the integrated diffraction profile but visible in the 2D pattern, a very faint WC peak at 41.6° (100) is observed. This may be an indication of the diffusion of W atoms through defects in the TiN layer, such as the grain boundaries associated with polycrystalline films. Such grain boundaries serve as high-diffusivity pathways in barrier materials compared to lattice diffusion and have been suggested as avenues for molybdenum carbide and silicide formation in the Mo/TiN/SiC system via the formation of Mo channels [21]. The weakening of the TiN signal after 24 h annealing may therefore be a result of TiN grain disassociation due to W diffusion. Nonetheless, neither W_2C nor W_5Si_3 peaks can be observed under these conditions, suggesting their formation in the presence of a TiN diffusion barrier is effectively suppressed.

To analyze the effect of annealing on the surface structure of the sputtered films, SEM images of the W/SiC and W/TiN/SiC samples as-deposited and annealed are presented in Fig. 2. First considering the set of W/SiC samples, the as-deposited film possesses a fine-grained structure, with small pores and groove lines in the film resulting from substrate defects. The 1 h annealed W/SiC reveals a homogenous, dense, small-grained structure, with no clear evidence of reaction, suggesting the silicide formation indicated in the XRD spectra is limited to the region near the interface. The localized nature of the interfacial reaction after 1 h is also observed upon visual inspection of the sample surface, which is mirror-like in nature and indistinguishable from the as-deposited sample. The 5 h annealed W/SiC shows an inhomogeneous surface characterized by light-colored, web-like agglomerations consisting of several small grains and indicates the reaction has extended to the surface of the 100 nm W film. The 24 h annealed W/SiC presents a severely reacted film with discontinuous agglomerations consisting of relatively large grains. Visually, the 5 and 24 h samples possess matte, rather than mirror-like, surfaces. In order to distinguish between the adjacent light and dark areas presented in the SEM images of the 5 and 24 h annealed samples (Fig. 2c and d), line scans using energy-dispersive x-ray spectroscopy (EDS) were conducted across these surfaces. Since the use of a 20 kV accelerating voltage results in the penetration of electrons through the sputtered film and an excitation volume inclusive of the SiC substrate, the following EDS analysis is viewed conservatively and qualitatively. Fig. 3 reveals that the overlying light regions in the SEM images of the 5 and 24 h annealed samples have a higher concentration of W and C, while the underlying dark regions have a higher concentration of Si. These line scans indicate that unreacted W and the W-based reaction products agglomerate to form island-like structures upon thermal annealing. Previous investigations into the surface morphology of the W on SiC system upon annealing have yielded a multitude of structures, including pores [4], small hillocks [8], large stacked grains [9,26], and islands [3,7], over a variety of conditions. The web-like agglomeration behavior observed for the 5 h sample under the present conditions (1273 K, 130 Pa Ar) is consistent with previous examinations by Thabethe, et al. upon thermal treatment of a thinner W film (65 nm) for less time (1 h) under similar conditions (1273 K, 10^{-1} Pa Ar) [7]. The transition to a discontinuous, large-grained structure upon further annealing is likely due to mixed contributions from further consumption of the unreacted W and grain growth.

For the W/TiN/SiC samples, the as-deposited film (Fig. 2e) is also observed to be fine-grained but with an improved film quality, having fewer voids and fainter grooves compared to the as-deposited W/SiC sample (Fig. 2a). After 1 h annealing, the W grains have grown larger and more rounded, though not as large or as dense as the corresponding W/SiC sample. The surface of the 5 h annealed sample is characterized by a small-dense grain structure with infrequent large grains. Further growth and densification are observed for the 24 h sample, with a transition to a more faceted-grain structure. In all cases, the W/TiN/SiC system maintains a relatively homogenous surface morphology without any significant modification to the W layer. This indicates that the agglomeration of W-containing species into islands observed in the W/SiC samples is induced by the interfacial reaction, rather than just thermal excursion, and highlights the improved stability offered by the TiN interlayer. This is further confirmed through visual inspection, as all annealed W/TiN/SiC samples retain the mirror-like surface quality of the as-deposited sample.

For several applications such as high-temperature electrical contacts and TECs, changes in the roughness of the W film during thermal excursion can impact device performance. As an example, the heat-to-electric conversion efficiency of TECs is quite sensitive to the inter-electrode spacing between the surfaces of a hot W electrode (electron emitter) and a parallel-placed, relatively cool electrode (electron collector) [27]. The optimal spacing was calculated to be a small as 900 nm, and in this context, local changes on the order of a micron could lead to reduced efficiency due to increased evanescent-wave heat transfer or thermal shorting. Understanding how the surface roughness of the W/SiC and W/TiN/SiC systems evolve under thermal excursion is

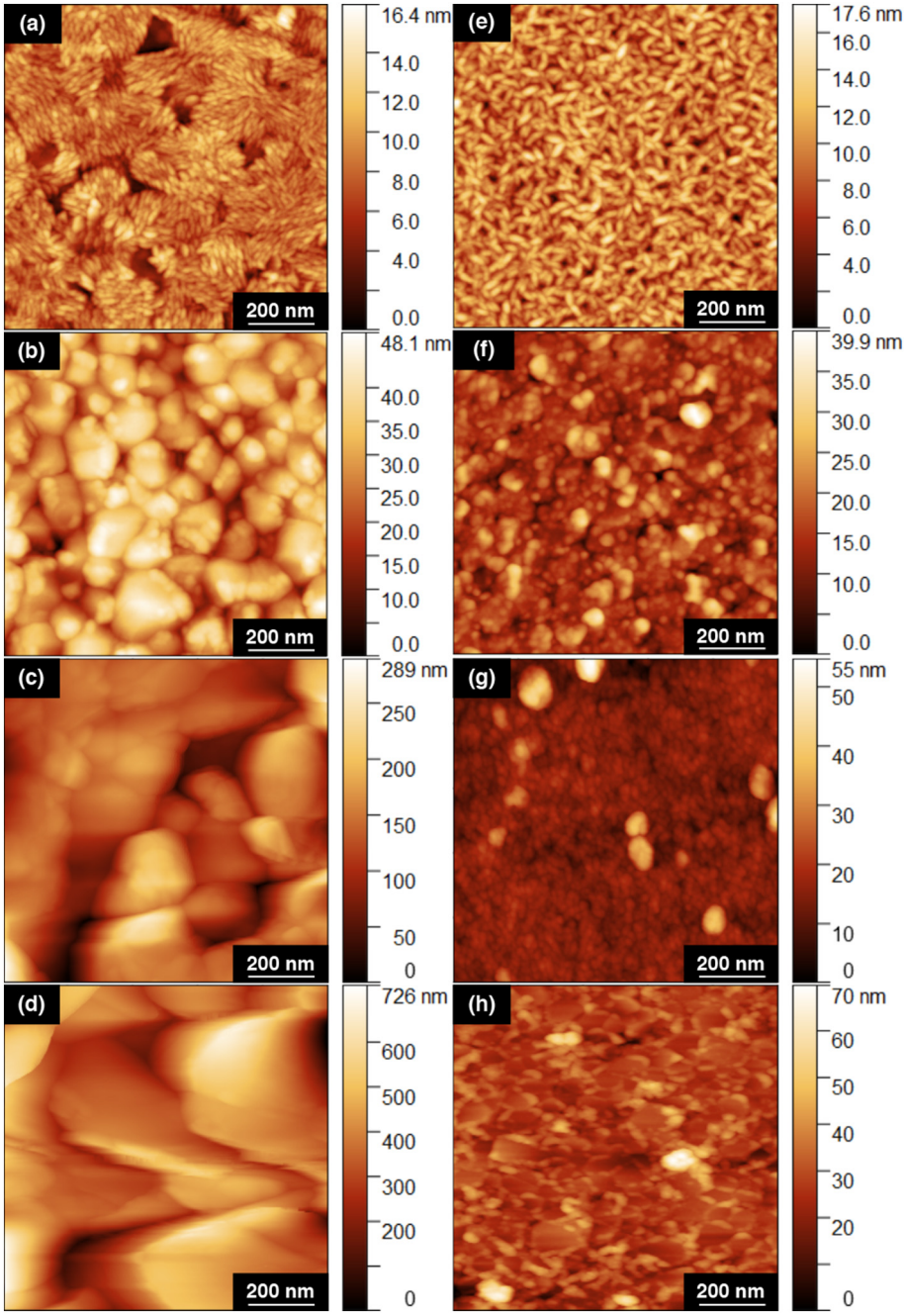

Fig. 4. (Left) AFM topographs of W/SiC samples (a) as-deposited and annealed at 1273 K for (b) 1 h, (c) 5 h, and (d) 24 h. (Right) AFM topograhs of W/TiN/SiC samples (e) as-deposited and annealed at 1273 K for (f) 1 h, (g) 5 h, and (h) 24 h.

Table 1
Roughness parameters for W/SiC and W/TiN/SiC samples from AFM scans.

	W/SiC		W/TiN/SiC	
Sample	R_a/nm	R_t/nm	R_a/nm	R_t/nm
As-deposited	2	16	2	18
1273 K, 1 h	6	48	4	40
1273 K, 5 h	30	289	3	55
1273 K, 24 h	84	726	5	70

critical to gauging their effectiveness as TEC emitter electrodes. Accordingly, the dependence of roughness on annealing time was evaluated using atomic force microscopy.

Fig. 4 presents the AFM images of W/SiC and W/TiN/SiC samples as-deposited and after annealing. The average roughness, R_a, and maximum height difference, R_t, values for each sample were calculated from representative 1 × 1 μm scans and are provided in Table 1. First considering the W/SiC system, the as-deposited and 1 h annealed samples have comparable R_a and R_t values, which is expected since the reaction after 1 h is limited to the region near the interface based on SEM images. For the 5 h annealed sample, R_a increases significantly due to the formation of the inhomogeneous web-like surface structure. After this time, R_t becomes greater than the film thickness due to contributions from parasitic grain growth and the consumption of the SiC substrate. The roughness of the W/SiC sample becomes more severe after 24 h, where R_a approaches the initial thickness of the W film and R_t approaches the size of the optimal TEC microgap. For the W/TiN/SiC system, the initial R_a is identical to that of the W/SiC system.

Depending on growth conditions, thicker TiN films possess large and faceted grain morphologies that affect the surface roughness of subsequently deposited films [28]. A 100 nm TiN film, however, is found to be sufficiently thick to suppress the reaction between W and SiC over the conditions examined without altering the initial R_a of the W layer. Upon annealing, small changes in both the R_a and the R_t values with time are observed and can be attributed to grain growth within the W layer. These values, however, are still comparable to that of the as-deposited film and are an order of magnitude less than that of the corresponding W/SiC samples. Additionally, no signs of delamination or fracture can be observed upon annealing. In this regard, the W/TiN/SiC system demonstrates excellent film stability and holds potential as an emitter electrode for micro-gap TEC devices.

4. Conclusion

The time-dependent behavior of the W on 4H-SiC(0001) system with and without a TiN diffusion barrier at elevated temperatures has been investigated. The progression of the solid-state reactions was evaluated by examining changes in the composition, surface morphology, and roughness through XRD, SEM, and AFM. For the W/SiC system, XRD analysis revealed the formation of W_5Si_3 after 1 h annealing and WC and W_2C after 5 h annealing. SEM and EDS analysis showed that the reaction between W and SiC induces the agglomeration of W-based species into an initially small-grained, web-like network and eventually into large-grained, isolated structures. This change in surface morphology led to an increase in the average surface roughness to a value on the order of the initial W film thickness. For the W/TiN/SiC system, XRD analysis revealed no formation of W_5Si_3 or W_2C species. Only a faint WC peak could be observed, which was attributed to the diffusion of W atoms through the grain boundaries of the TiN layer. SEM and AFM analysis showed minimal grain growth of the W layer upon annealing and inconsequential changes in surface morphology or roughness. The additional stability in composition and surface characteristics at high temperatures brought about by the incorporation of a TiN interlayer warrants further consideration of the W/TiN/SiC system as a TEC emitter electrode.

Acknowledgements

This work was supported by the Advanced Research Projects Agency-Energy (ARPA-E), U.S. Department of Energy, under Award No. DE-AR0000664. The authors also thank Dung-Sheng Tsai and Chuan-Pei Lee for fruitful discussions. Sputtering was performed in the UC Berkeley Marvell Nanofabrication Laboratory. Work at the Molecular Foundry was supported by the Office of Science, Office of Basic Energy Sciences, of the U.S. Department of Energy under Contract No. DE-AC02-05CH11231.

References

[1] S.J. Son, K.H. Park, Y. Katoh, A. Kohyama, Interfacial reactions and mechanical properties of W-SiC in-situ joints for plasma facing components, J. Nucl. Mater. 329–333 (2004) 1549–1552, https://doi.org/10.1016/j.jnucmat.2004.04.285.

[2] G.H. Gubbels, R. Metselaar, E. Penders, L.R. Wolff, Combustion heated thermionic energy converter, 21st Intersoc. Energy Convers. Eng. Conf, 1986, pp. 1343–1345 San Diego, CA, USA.

[3] F. Goesmann, R. Schmid-Fetzer, Stability of W as electrical contact on 6HSiC: phase relations and interface reactions in the ternary system WSiC, Mater. Sci. Eng. B 34 (1995) 224–231, https://doi.org/10.1016/0921-5107(95)01311-3.

[4] J. Rogowski, A. Kubiak, Effects of annealing temperature on the structure and electrical properties of tungsten contacts to n-type silicon carbide, Mater. Sci. Eng. B 191 (2015) 57–65, https://doi.org/10.1016/j.mseb.2014.10.015.

[5] W.F. Seng, P.A. Barnes, Calculations of tungsten silicide and carbide formation on SiC using the Gibbs free energy, Mater. Sci. Eng. B 72 (2000) 13–18, https://doi.org/10.1016/S0921-5107(00)00457-8.

[6] L. Baud, C. Jaussaud, R. Madar, C. Bernard, J.S. Chen, M.A. Nicolet, Interfacial reactions of W thin film on single-crystal (001) β-SiC, Mater. Sci. Eng. B 29 (1995) 126–130, https://doi.org/10.1016/0921-5107(94)04017-X.

[7] T.T. Thabethe, T.T. Hlatshwayo, E.G. Njoroge, T.G. Nyawo, T.P. Ntsoane, J.B. Malherbe, Interfacial reactions and surface analysis of W thin film on 6H-SiC, Nucl. Inst. Methods Phys. Res. B 371 (2016) 235–239, https://doi.org/10.1016/j.nimb.2015.10.063.

[8] T.T. Thabethe, T.T. Hlatshwayo, E.G. Njoroge, T.G. Nyawo, J.B. Malherbe, The effect of thermal annealing in a hydrogen atmosphere on tungsten deposited on 6H-SiC, Vacuum 129 (2016) 161–165, https://doi.org/10.1016/j.vacuum.2016.03.018.

[9] T.T. Thabethe, E.G. Njoroge, T.T. Hlatshwayo, T.P. Ntsoane, J.B. Malherbe, Surface and interface structural analysis of W deposited on 6H-SiC substrates annealed in argon, RSC Adv. 7 (2017) 2–7, https://doi.org/10.1039/C6RA24825J.

[10] K. Park, K. Kim, Effect of annealing of titanium nitride on the diffusion barrier property in Cu metallization, J. Electrochem. Soc. 142 (1995) 3109–3115, https://doi.org/10.1149/1.2048697.

[11] M. Moriyama, T. Kawazoe, M. Tanaka, M. Murakami, Correlation between microstructure and barrier properties of TiN thin films used Cu interconnects, Thin Solid Films 416 (2002) 136–144, https://doi.org/10.1016/S0040-6090(02)00602-8.

[12] L. Gao, J. Gstöttner, R. Emling, M. Balden, C. Linsmeier, A. Wiltner, W. Hansch, D. Schmitt-Landsiedel, Thermal stability of titanium nitride diffusion barrier films for advanced silver interconnects, Microelectron. Eng. 76 (2004) 76–81, https://doi.org/10.1016/j.mee.2004.07.020.

[13] K. Suguro, Y. Nakasaki, T. Yoshii, T. Itoh, Barrier metal between tungsten and silicon for high temperature processing, Appl. Surf. Sci. 41–42 (1989) 277–281, https://doi.org/10.1016/0169-4332(89)90070-6.

[14] L.V. Strashinskaya, An investigation of the compatibility of refractory compounds of titanium with refractory metals in vacuum, Mater. Sci. 12 (1977) 330–332, https://doi.org/10.1007/BF00722713.

[15] R.C. Glass, L.M. Spellman, R.F. Davis, Low energy ion-assisted deposition of titanium nitride ohmic contacts on alpha (6H)-silicon carbide, Appl. Phys. Lett. (1991) 2868–2870, https://doi.org/10.1063/1.105836.

[16] R.C. Glass, L.M. Spellman, S. Tanaka, R.F. Davis, Chemical and structural analyses of the titanium nitride/alpha (6H)-silicon carbide interface, J. Vac. Sci. Technol. A 10 (1992) 1625–1630, https://doi.org/10.1116/1.578033.

[17] A.A. Iliadis, S.N. Andronescu, K. Edinger, J.H. Orloff, R.D. Vispute, V. Talyansky, R.P. Sharma, T. Venkatesan, M.C. Wood, K.A. Jones, Ohmic contacts to p-6H-SiC using focused ion-beam surface-modification and pulsed laser epitaxial TiN deposition, Appl. Phys. Lett. (1998) 3545–3547, https://doi.org/10.1063/1.122802.

[18] L. Hultman, H. Ljungcrantz, C. Hallin, E. Janzén, J.E. Sundgren, B. Pécz, L.R. Wallenberg, Growth and electronic properties of epitaxial TiN thin films on 3C-SiC(001) and 6H-SiC(0001) substrates by reactive magnetron sputtering, J. Mater. Res. (1996) 2458–2462, https://doi.org/10.1557/JMR.1996.0309.

[19] X. Shi, M. Wang, S. Zhang, Q. Zhang, Fabrication and properties of W-20Cu alloy reinforced by titanium nitride coated SiC fibers, Int. J. Refract. Met. Hard Mater. (2013) 60–65, https://doi.org/10.1016/j.ijrmhm.2013.02.002.

[20] S. Brust, A. Röttger, W. Theisen, New wear-resistant materials for mining applications, Int. Conf. Stone Concr. Mach, 2015, pp. 272–280, , https://doi.org/10.13154/icscm.3.2015.272-280.

[21] J. Roger, F. Audubert, Y. Le Petitcorps, Reactivity of M/TiN/SiC systems (M = W and Mo) at high temperature, J. Mater. Sci. 45 (2010) 3073–3079, https://doi.org/10.1007/s10853-010-4314-x.

[22] G. Fitzpatrick, J. Lawless, Y. Nikolaev, S. Yeremin, A. Klinkov, J. McVey, Demonstration of close-spaced thermionic converters, Proc. 28th Intersoc. Energy Convers. Eng. Conf. 1993, pp. 573–580.

[23] G. Gärtner, P. Geittner, H. Lydtin, A. Ritz, Emission properties of top-layer scandate cathodes prepared by LAD, Appl. Surf. Sci. 11–17 (1997), https://doi.org/10.1016/S0169-4332(96)00698-8.

[24] J.A. Michel, V.S. Robinson, L. Yang, S. Sambandam, W. Lu, T. Westover, T.S. Fisher, C.M. Lukehart, Synthesis and characterization of potassium metal/graphitic carbon nanofiber intercalates, J. Nanosci. Nanotechnol. (2008) 1942–1950, https://doi.org/10.1166/jnn.2008.308.

[25] J.H. Lee, I. Bargatin, B.K. Vancil, T.O. Gwinn, R. Maboudian, N.A. Melosh, R.T. Howe, Microfabricated thermally isolated low work-function emitter, J. Microelectromech. Syst. 23 (2014) 1182–1187, https://doi.org/10.1109/JMEMS.2014.2307882.

[26] S.M. Tunhuma, M. Diale, M.J. Legodi, J.M. Nel, T.T. Thabete, F.D. Auret, Defects induced by solid state reactions at the tungsten-silicon carbide interface, J. Appl. Phys. 123 (2018) 161565, , https://doi.org/10.1063/1.5011242.

[27] J.H. Lee, I. Bargatin, N.A. Melosh, R.T. Howe, Optimal emitter-collector gap for thermionic energy converters, Appl. Phys. Lett. 100 (2012) 173904, , https://doi.org/10.1063/1.4707379.

[28] S. Mahieu, P. Ghekiere, D. Depla, R. De Gryse, Biaxial alignment in sputter deposited thin films, Thin Solid Films 515 (2006) 1229–1249, https://doi.org/10.1016/j.tsf.2006.06.027.